

Investigation on the mechanical performance of mono-material vs multi-material interface geometries using fused filament fabrication

Damira Dairabayeva, Asma Perveen and Didier Talamona

Department of Mechanical and Aerospace Engineering, School of Engineering and Digital Sciences, Nazarbayev University, Astana, Kazakhstan

Abstract

Purpose – Currently on additive manufacturing, extensive research is directed toward mitigating the main challenges associated with multi-material in fused filament fabrication which has a weak bonding strength between dissimilar materials. Low interfacial bonding strength leads to defects, anisotropy and temperature gradient in materials which negatively impact the mechanical performance of the multi-material prints. The purpose of this study was to assess the performance of different interface geometry designs in terms of the mechanical properties of the specimens.

Design/methodology/approach – Tensile test specimens were printed using: mono-material without a boundary interface, mono-material with the interface geometries (Face-to-face; U-shape; T-shape; Dovetail; Encapsulation; Mechanical interlocking; and Overlap) and multi-material with the interface geometries. The materials chosen with high and low compatibility were Tough polylactic acid (PLA) and TPU.

Findings – The main results of this study indicate that the interface geometries with the mechanical constriction between materials provide better structural integrity to the specimens. Moreover, in the case of the mono-material parts, the most effective interface design was the mechanical interlocking for both Tough PLA and TPU. On the other hand, in the case of multi-material specimens, the encapsulation showed the highest ultimate tensile strength, whereas the overlap and T-shape presented more robust bonding.

Originality/value – This study examines the mechanical performance, particularly tensile strength, strain at break, Young's modulus and yield strength of different interface designs which were not studied in the previous studies.

Keywords Additive manufacturing, Multi-material fused filament fabrication, Interface designs, Interfacial bonding, Boundary interface

Paper type Research paper

1. Introduction

Additive manufacturing (AM) or rapid prototyping (RP) is the layer-based fabrication process that emerged in the late 1980s. Although AM was initially introduced for the fabrication of mono-material parts, because of the development of AM technologies in conjugation with industrial needs for composite components, multi-material three-dimensional (3D) printers started to emerge on the market. The printers enable the incorporation of different materials to enhance the functional performance and complexity of AM-fabricated parts (Amancio-Filho and dos Santos, 2009).

One of the most affordable and widely used AM technologies is fused deposition modeling (FDM®), proposed originally by Stratasy Inc. FDM®, which is also commonly known as fused filament fabrication (FFF). In FDM®, the thermoplastic polymers are extruded through a heated nozzle to fabricate the part layer by layer (Jasveer and Jianbin, 2018).

However, the main challenge associated with multi-material FFF is the weak bonding strength between materials, which is mainly because of the differences in

physical and chemical properties between dissimilar materials. The boundary interface is a physical discontinuity and a weak point in the specimen. Low interfacial bonding strength results in the formation of defects that affect the overall mechanical performance of the printed parts. The weak bonding is also because of anisotropy and temperature gradient during printing in materials. One of the possible approaches to enhance the mechanical strength of multi-material parts is the modification of interface geometries that may additionally provide a mechanical interlocking for example (Zheng *et al.*, 2021).

The boundary interface is a physical discontinuity and a weak point in the specimen. Hence, numerous studies focus on

© Damira Dairabayeva, Asma Perveen and Didier Talamona. Published by Emerald Publishing Limited. This article is published under the Creative Commons Attribution (CC BY 4.0) licence. Anyone may reproduce, distribute, translate and create derivative works of this article (for both commercial and non-commercial purposes), subject to full attribution to the original publication and authors. The full terms of this licence may be seen at <http://creativecommons.org/licenses/by/4.0/legalcode>

This research was funded under the target program (no. OR07665556) for project entitled “Additive production systems and metal powders for Kazakhstan industry”, by the Ministry of Industry and Infrastructure Development of the Republic of Kazakhstan.

Received 6 July 2022
Revised 23 September 2022
23 November 2022
Accepted 6 December 2022

The current issue and full text archive of this journal is available on Emerald Insight at: <https://www.emerald.com/insight/1355-2546.htm>



Rapid Prototyping Journal
29/11 (2023) 40–52
Emerald Publishing Limited [ISSN 1355-2546]
[DOI 10.1108/RPJ-07-2022-0221]

improving interfacial bonding between different materials. Kim *et al.* (2017) studied the cases of fracture at the interface of polylactic acid (PLA) and acrylonitrile butadiene styrene (ABS). It was found that the structural arrangement affects the tensile strength of the part, and the addition of horizontal layers improves the adhesion between materials. Lin *et al.* (2018) proposed a single-layer temperature-adjusting transition method to increase the bonding between materials with different melting temperatures. In this method, the first layer of the second material is deposited at a higher nozzle temperature than the nozzle temperature for the consecutive layers. Fernández *et al.* (2019) found that the minimum degree of overlapping between two materials causes a significant increase in the strength of the sample.

Several studies focused on the effect of printing and slicing parameters on the interfacial bonding between two materials. Yin *et al.* (2018) examined the bonding between ABS and TPU and concluded that the increase in the building stage of the temperature resulted in the highest impact, while the printing speed had the smallest effect on the improvement of bonding strength. Tamburrino *et al.* (2019) identified that the printing order and infill density affect the bonding, while the creation of mechanical interface geometry between materials increases the tensile strength of the parts.

Nace *et al.* (2021) performed a comparative analysis of TPU's compressive mechanical properties of 3D printed parts for four infill patterns and infill density for "comfort applications." Concentric, cross, cross 3D and gyroid infill patterns were considered. It was found that, as expected, when the infill density was increased, the stiffness of the part also increases. While the results for the infill pattern were more complicated to analyze, it was recommended to use gyroid as a replacement for viscoelastic polyurethane foams. This research helped to develop 3D printed parts with specific stiffness and damping coefficient for the control of vibrations.

Moreover, recent investigations have focused on the interlocking patterns and gradient transition between different materials. Kuipers *et al.* (2022) proposed an interlaced topologically interlocking lattice method, which allows the locking of three axes of space and satisfies the continuity constraint of extrusion. Stoner *et al.* (2018) examined the functionally graded materials characterized by changing composition in a discrete or continuous fashion throughout the volume of the specimen. The experiment resulted in the design of the bi-continuous material interface using a triply periodic minimal surface. However, the production of functionally graded materials is still limited to a few AM processes such as directed energy deposition and material jetting. Hasanov *et al.* (2020) compared the strength of the gradient transition multi-material parts of PC and ABS with the butt-jointed and interlocked specimens. The conclusion was that the gradient transition provides and reduces the interface stress concentrations. Nevertheless, the gradient transition between materials might not be possible for many commercial desktop printers. Vu *et al.* (2018) subjected the multi-material specimens of soft and stiff materials to the T-peel test and concluded that the gradient interface increased the peel resistance of the specimens by roughly 62% in comparison to the direct transition.

However, few studies investigated the effect of interface geometries between materials on the mechanical performance of the parts manufactured using FFF. Therefore, this work aims to compare the mechanical properties of interface designs between the set of materials with high and low chemical affinity. The study not only is in line with the work done by Lopes *et al.* (2018) and Ribeiro *et al.* (2018) but also provides an evaluation of the additional interface geometries.

2. Methodology

This section describes the stages of the experiment, the selected materials and printing process parameters, as well as the specifications of the interface geometries.

2.1 Experimental procedure

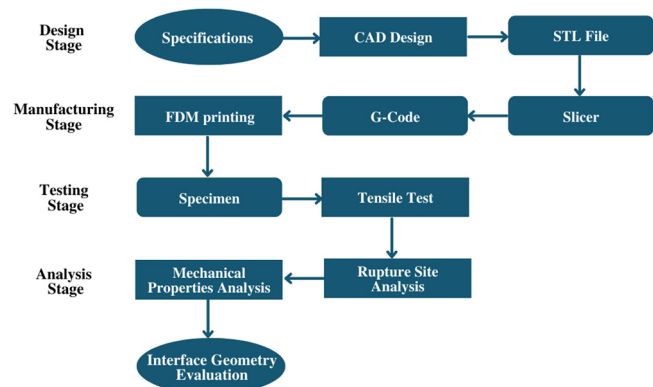
This study was conducted in several stages as shown in Figure 1. The flowchart illustrates the four main stages such as design, manufacturing, testing and analysis. First, the specifications, namely, the materials and interface geometries, were selected. The models were designed using SolidWorks 2021, a computer-aided design software, and transformed into the stereolithography format file, which defines the surface geometry of the model. Second, the model was sliced in the computer software and converted into the G-Code format. The specimens were manufactured using the FFF printer, Ultimaker S3. Third, the printed specimens were subjected to a tensile test to failure. Finally, the various designs were evaluated based on the analysis of their rupture sites and mechanical properties.

2.2 Materials

The materials used in this study were Ultimaker Black Tough PLA and Ultimaker Blue TPU95A. Tough PLA refers to a technical PLA filament characterized by high impact resistance and toughness comparable with ABS. The material offers greater machinability than PLA, higher stiffness than ABS and neither warpage nor delamination (Ultimaker, 2023a, 2023b). TPU is a thermoplastic elastomer that has high rubber-like flexibility, increased wear and tear resistance and good corrosion resistance to common chemicals (Ultimaker, 2023a, 2023b).

These materials were selected because of their low chemical affinity and allowing the combinations of rigid and flexible

Figure 1 Stages of the experiment



parts. These two materials would allow the development of composite parts that have strength and damping properties that can be adjusted to reduce vibrations. Single-material specimens were printed using both Tough PLA and TPU as references and were manufactured with and without (monoblock) an interface. In multi-material models, the parts with outgoing (male) features were chosen to be Tough PLA.

To summarize, the following combinations were examined in this study:

- Mono-material (monoblock) specimens: Tough PLA and TPU;
- Mono-material specimens with an interface geometry: Tough PLA–Tough PLA and TPU–TPU; and
- Multi-material specimens: Tough PLA–TPU.

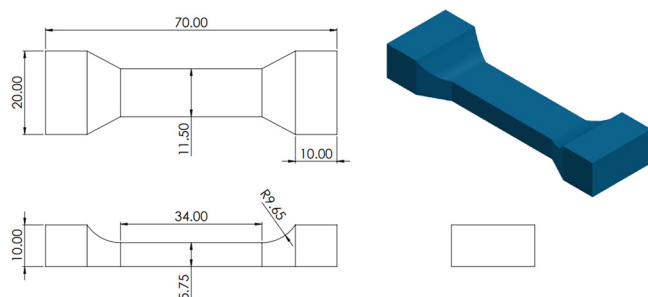
2.3 Interface geometries

The original model of the specimen that was subjected to tensile tests is shown in [Figure 2](#). The main advantage of this particular specimen is the visual representation of the initial distance between grips for tensile tests. The mono-material specimens without a boundary interface were printed as references to study the effect of the boundary interface on the structural integrity of the parts.

The interface designs tested in the study are shown in [Figure 3](#). The presence of the boundary was expected to have a negative impact on the mechanical properties of the specimens. All geometries were printed with mono-material and multi-material pairs:

- The face-to-face interface refers to the butt-jointed pair of materials where two parts are simply connected end-to-end at the faces. The boundary is located at the midsection of the specimen. The bonding depends only on the adhesive forces between the materials.
- The U-shape is similar to the insert with no constriction from the perspective of axial load. Hence, this design relies mainly on the chemical compatibility between materials.
- The T-shape is characterized by the true mechanical locking system which can constrict the detachment between materials.
- The dovetail is considered to be the simplified version of the previous geometry. The design is dependent on both chemical and mechanical bonds between the parts of the specimens.
- The encapsulation has one material printed in a rectangular shape enclosed by another material.

Figure 2 Dimensions of the tensile test specimen



- The mechanical interlocking refers to the design similar to the U-shape geometry, but the outgoing feature is enclosed with the walls and top/bottom layers of the specimen.
- The overlap has each layer of one material alternating with another material. The length of the section in the middle where the overlapping occurs is 3 mm. The overlap of materials creates friction between layers which can enhance the bonding.

The face-to-face interface was selected to establish a reference for comparison with other designs. The U-shape, T-shape and dovetail geometries were based on the study by [Ribeiro et al. \(2018\)](#). The encapsulation was chosen to identify which material would demonstrate dominance under the tensile stress. The mechanical interlocking and the overlap were designed because of the work of [Tamburrino et al. \(2019\)](#) and [Fernández et al. \(2019\)](#), respectively. Although these designs were studied before, a more comprehensive investigation of mechanical properties and comparison between them are required.

2.4 Printing process parameters

The specimens were fabricated using Ultimaker S3, the desktop printer capable of dual extrusion. Ultimaker Cura 4.11.0 software was used to set up the parts for printing. The printing conditions detailed in [Table 1](#) were applied for mono-material as well as multi-material specimens with high and low chemical affinity.

2.5 Tensile test

The specimens were subjected to the tensile test using a universal testing machine, Tinius Olsen equipment. The force was applied in the normal direction to the interface plane as shown in [Figure 4](#). All tests were performed at the crosshead speed of 10 mm/min. Three replicas of each mono-material and multi-material interface geometries were printed and tested. The mechanical properties of specimens such as tensile strength, strain at break, Young's modulus, yield strength and the location of the fracture site were recorded.

3. Results and discussion

This section presents the experimental results and findings. Particularly, the analysis of the rupture sites and variations of the mechanical properties of the specimens with different interface geometries is discussed.

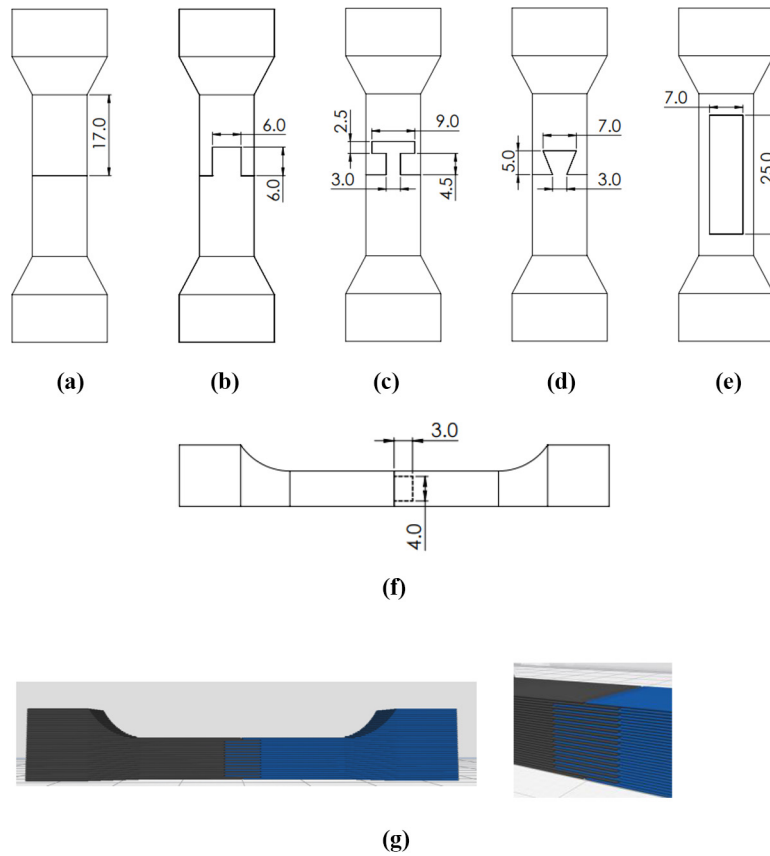
3.1 Rupture sites

A preliminary study of the fracture sites was conducted before the analysis of the tensile test results. The location of the rupture sites is depicted in [Figures 5, 6, 7 and 8](#).

As shown in [Figure 5](#), the rupture in the mono-material specimens without any interface of both Tough PLA and TPU occurred in the weakest point which was the vicinity of the jaws or near the increases of the cross-section.

Focusing on mono-material with an interface, Tough PLA–Tough PLA specimens ([Figure 6](#)), the rupture by detachment along the geometry lines was found only in the face-to-face interface. For the encapsulation case, the fracture occurred at the boundary interface near a jaw.

Figure 3 Interface designs



Notes: (a) Face-to-face; (b) U-shape; (c) T-shape; (d) dovetail; (e) encapsulation; (f) mechanical interlocking; (g) overlap

Table 1 Printing process parameters

Parameters	Value
Layer thickness	0.2 mm
Infill	100%
Infill pattern	Grid
Print speed	20 mm/s
Bed temperature	60°C
Nozzle diameter	0.4 mm
Tough PLA nozzle temperature	215°C
TPU nozzle temperature	225°C

In the U-shape, dovetail and T-shape specimens, the rupture site was partially located at the interface line. However, the parts of the receiving geometry were still attached to the outgoing feature because of the high compatibility between materials.

The overlap and mechanical interlocking specimens failed because of the breakage of geometric elements which indicates the strong adhesion between the parts.

Similar behavior as Tough PLA was observed for the mono-material TPU with an interface. As can be seen in [Figure 7](#),

Figure 4 Set up of the tensile test

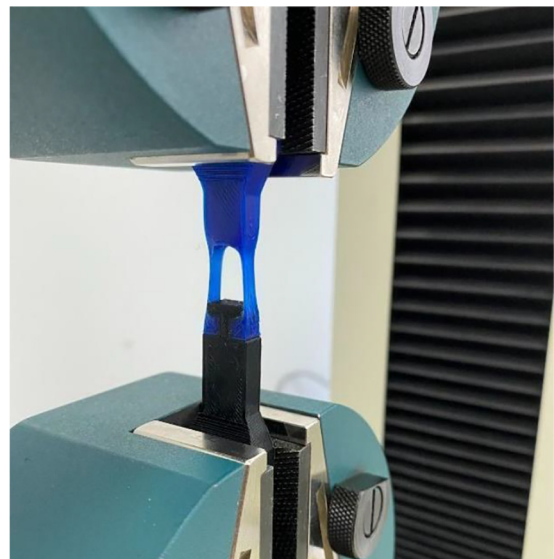
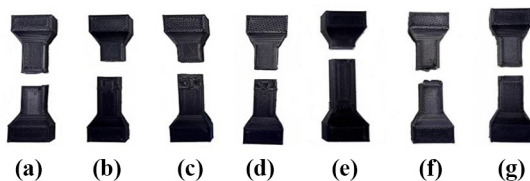


Figure 5 Rupture sites of the mono-material specimens without a boundary interface



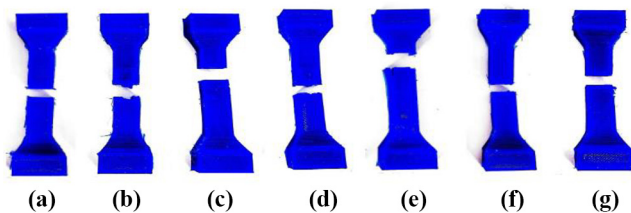
Notes: (a) Tough PLA; (b) TPU

Figure 6 Rupture sites of the Tough PLA–Tough PLA specimens



Notes: (a) Face-to-face; (b) U-shape; (c) T-shape; (d) dovetail; (e) encapsulation; (f) mechanical interlocking; (g) overlap

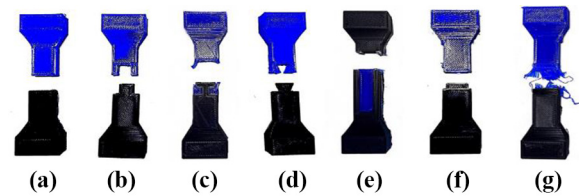
Figure 7 Rupture sites of the TPU–TPU specimens



Notes: (a) Face-to-face; (b) U-shape; (c) T-shape; (d) dovetail; (e) encapsulation; (f) mechanical interlocking; (g) overlap

almost all specimens for the TPU–TPU combination demonstrated a similar pattern to Tough PLA–Tough PLA except for the dovetail and U-shape geometries. The rupture of these two designs occurred across the “bottom” interface (at the root of the extruded “U” or dovetail). The breakage of the geometric elements indicates the high adhesion between the two parts of the sample. The rupture site of the design is in congruity with the results of Ribeiro *et al.* (2018). The reason is that the weakest point corresponding to the fracture site is not located only along the interface line. This means that the

Figure 8 Rupture sites of the Tough PLA–TPU specimens



Notes: (a) Face-to-face; (b) U-shape; (c) T-shape; (d) dovetail; (e) encapsulation; (f) mechanical interlocking; (g) overlap

bonding between the two parts of the specimen is robust because of the selected design. This might suggest the high bonding strength and effectiveness of these interface geometries in addition to the mechanical interlocking and overlap designs.

Figure 8 shows the fracture sites of the multi-material interface geometries that differ from their Tough PLA–Tough PLA and TPU–TPU counterparts.

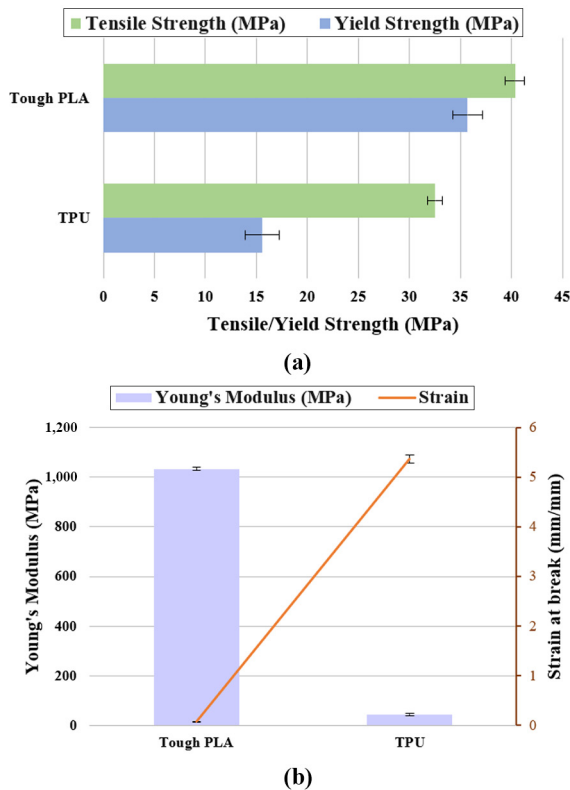
For the overlap specimens, the materials were partially joined at the interface after the rupture, as each layer of the flexible material was followed by the stiff material. The fracture started from the outer surfaces (top/bottom layers) of the sample being detached. This pattern sustained the strong attachment between the materials, as a substantial amount of debris of flexible material was seen in the adjacent part after the rupture.

The T-shape specimen ruptures similarly to the mono-material specimens of the same design because of the presence of true mechanical constriction between the materials, which prevents detachment. This cross-section was also the weakest of the composite. In the encapsulation specimen, the TPU part remained almost intact, and only a few pieces of debris were found in the corresponding stiff part after the rupture. These specimens also failed at the weakest cross-section. The mechanical interlocking, U-shape, dovetail failed by the slipping away of the flexible material. This detachment behavior confirms the low chemical affinity between Tough PLA and TPU. Finally, a clear separation in the boundary interface of the face-to-face interface specimen was observed as expected. Based on this initial visual study of the multi-material interfaces, the overlap and T-shape geometries demonstrated strong adhesion in comparison to other specimens.

3.2 Mechanical properties of mono-material specimens

The experimental results for mono-material specimens without the boundary interface for tensile strength, yield strength, Young’s modulus and strain at break are shown in Figures 9(a) and 9(b), respectively. As shown in Table 2, Young’s modulus was 1,033.6 MPa and yield strength 35.7 MPa for Tough PLA specimens. Their properties were significantly higher than the corresponding values of TPU specimens 44.8 MPa and 15.5 MPa, for Young’s modulus and yield strength, respectively, as Tough PLA is considered to be a rigid material when compared to an elastomer (TPU). On the contrary, the strain at break of TPU was higher because of the flexibility of the material, whereas the tensile strength of both materials was

Figure 9 Single-material specimens without a boundary interface



Notes: (a) Tensile and Yield Strength;
(b) Young's modulus and Strain

comparatively close because of the larger elongation range provided by the TPU.

The Tough PLA–Tough PLA and TPU–TPU pairs were printed to investigate the effect of geometry patterns on the materials with the highest compatibility. It can be observed that the presence of a boundary interface negatively affects the mechanical properties of the specimens. These results agree with the findings of Lopes *et al.* (2018).

The average values of mechanical properties for the mono-material Tough PLA specimens are summarized in Table 3.

Figure 10(a) shows the tensile strength of the mono-material Tough PLA specimens. Interestingly, the tensile strength of the face-to-face interface (25.0 MPa) is comparable to the results of the other boundary geometries and slightly higher than the T-shape and dovetail interface. The low level of variation between these interfaces can be attributed to the high compatibility of the same materials.

The highest strength was recorded for the overlap (29.3 MPa) and mechanical interlocking (29.14 MPa). These results

are consistent with the previous analysis of the rupture sites. The failure of both designs was because of the breakage of geometric elements at the interface which suggested strong bonding between the complementary parts.

The lower values observed for the dovetail, U-shape (22.6 MPa) and T-shape (22.5 MPa) cases seem to be in line with the rupture site analysis, as the fracture occurred at the major interface line.

As for the yield strength indicated in Figure 10(a), the variations in the values also seem to be dependent on the interface design choice. The pattern is similar to the one observed in the tensile strength. The yielding at higher values of stress close to the ultimate tensile strength is because of the brittle nature of Tough PLA material.

Figure 10(b) illustrates Young's modulus values of the specimens. The specimens exhibited a brittle fracture because of the rigidity of the material. Therefore, the interface geometries with strong locking mechanisms such as the overlap (1,022.8 MPa) and mechanical interlocking (958.03 MPa) exhibit the highest values of Young's modulus.

Based on Figure 10(b), the strain at break was highest for the mechanical interlocking (0.0439) and T-shape (0.0404) specimens, as their geometric elements enabled further elongation without immediate detachment. On the other hand, the face-to-face interface (0.0319) demonstrated the lowest strain values because of the simple butt-joined design and the occurrence of rupture exactly along the interface line.

Table 4 shows the decreases in the percentage of the mechanical properties because of the presence of the boundary interface on the mechanical performance of the mono-material Tough PLA specimens. All interface geometries resulted in the decrease of all four mechanical properties. The performance of the geometries was evaluated based on the level of variation from the mono-material specimens without an interface.

The most effective design is the overlap which showed the lowest variation in terms of the tensile strength (27.3%), yield strength (23.2%) and Young's modulus (1.0%) as well as the moderate strain at break variation (53.5%). The second-best interface is the mechanical interlocking with the comparable tensile and yield strength variation and lower variation in the strain at break (46.7%) but higher variation in Young's modulus (7.3%). The highest variation in the strain at break is shown by the face-to-face interface (61.3%). Moreover, the highest Young's modulus variation is observed in the encapsulation (18.1%). The worst interface is T-shape with the highest variation in the tensile strength (44.1%) and yield strength (42.2%).

The Tukey test is a post hoc analysis in one-way ANOVA used to compare each pair of factors and examine whether their means are statistically significant. In this method, the mean of each factor level is compared to the every other one and the

Table 2 Mechanical properties of mono-material specimens

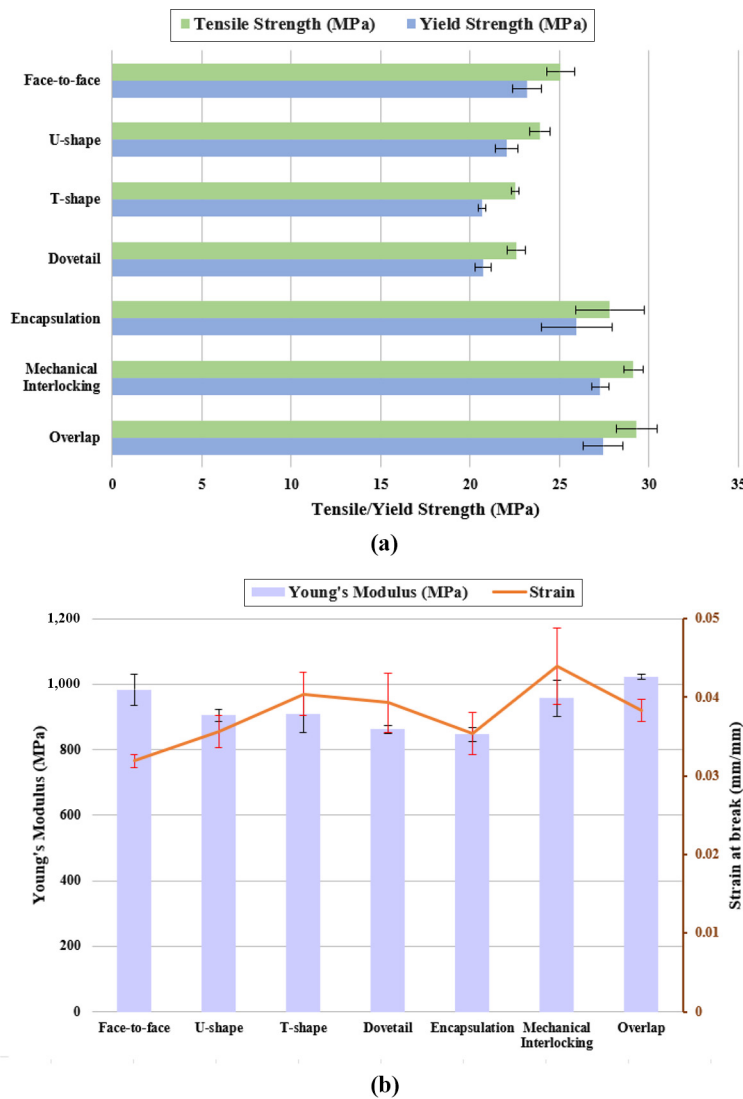
Materials	Tensile strength (MPa)		Yield strength (MPa)		Young's modulus (MPa)		Strain at break	
	Mean	SD	Mean	SD	Mean	SD	Mean	SD
Tough PLA	40.3	1.0	35.7	1.5	1,033.6	7.6	0.0824	0.003
TPU	32.5	0.8	15.5	1.9	44.8	6.8	5.4	0.09

Table 3 Mechanical properties of the Tough PLA–Tough PLA specimens

Interface geometries	Tensile strength (MPa)			Yield strength (MPa)			Young’s modulus (MPa)			Strain at break		
	Mean	SD	Group	Mean	SD	Group	Mean	SD	Group	Mean	SD	Group
Face-to-face	25.0	0.8	A	23.2	0.8	A	983.4	47.0	A/B	0.0319	0.0007	A
U-shape	23.9	0.6	A	22.1	0.6	A	904.7	17.1	B/C/D	0.0356	0.0020	A/B
T-shape	22.5	0.2	A	20.7	0.2	A	910.4	56.4	B/C/D	0.0404	0.0027	B/C
Dovetail	22.6	0.5	A	20.7	0.5	A	862.3	13.1	C/D	0.0393	0.0038	A/B/C
Encapsulation	27.8	1.9	B	26.0	2.0	B	846.7	20.8	D	0.0354	0.0027	A/B
Mechanical interlocking	29.1	0.5	B	27.3	0.5	B	958.0	55.2	A/B/C	0.0439	0.0048	C
Overlap	29.3	1.1	B	27.4	1.1	B	1022.8	6.9	A	0.0383	0.0016	A/B/C

Note: Interface geometries that do not share any letter have significantly different means

Figure 10 Tough PLA–Tough PLA specimens



Notes: (a) Tensile and Yield Strength; (b) Young’s modulus and Strain

95% confidence intervals are created for all pairwise differences (Minitab, 2022).

The results of the confidence intervals for the difference between the mean of each interface and control level are used by

the Minitab software to group the interfaces. First, the first letter A is assigned to the control level. In case a confidence interval of a pairwise comparison contains zero, the same letter is assigned to the level. Otherwise, no letter is given to the level (Minitab, 2021).

Table 4 Effect of the interface geometries on the mechanical properties of mono-material Tough PLA specimens

Interface geometries	Tensile strength		Yield strength		Young's modulus		Strain at break	
	Variation (%)	<i>p</i> -value	Variation (%)	<i>p</i> -value	Variation (%)	<i>p</i> -value	Variation (%)	<i>p</i> -value
Face-to-face	38.0	0.00003	35.2	0.00018	4.8	0.14167	61.3	0.00001
U-shape	40.7	0.00001	38.3	0.00011	12.5	0.00028	56.8	0.00002
T-shape	44.1	0.00001	42.2	0.00005	11.9	0.01996	51.0	0.00005
Dovetail	44.0	0.00001	42.0	0.00006	16.6	0.00004	52.3	0.00010
Encapsulation	31.0	0.00055	27.3	0.00226	18.1	0.00013	57.0	0.00003
Mechanical interlocking	27.8	0.00006	23.7	0.00062	7.3	0.07795	46.7	0.00030
Overlap	27.3	0.00022	23.2	0.00133	1.0	0.14451	53.5	0.00002

Note: The means of interface geometries are compared to the monoblock Tough PLA to obtain the variation percentage and *p*-value

The results were grouped to identify the statistical significance between the interface geometries. The grouping allows a brief demonstration of the statistical difference through the use of different letters to denote the means which are significantly different.

As shown in Table 3, the interface designs such as face-to-face, U-Shape, T-Shape and dovetail share the letter (A) for the tensile strength, which means that the difference in their means is not statistically significant. The same principle applies to the encapsulation, mechanical interlocking and overlap geometries, which belong to the group (B). On the contrary, the means that do not share the same letter are significantly different at a significance level of 0.05.

The encapsulation, mechanical interlocking and overlap share a letter (B), indicating a significantly higher mean for the tensile and yield strength than the designs of other groups (A). The overlap (A) and encapsulation (D) are the only interfaces with different letters, while others share two or three letters. In the case of strain at break, the face-to-face (A) and mechanical interlocking (C) have significantly different means.

The combination of letters such as A/B or A/B/C refers to the means in the transitional range. For example, the strain at break of the U-shape interface (A/B) is in both groups A and B. This overlap means that there is no significant difference in means of the U-shape and face-to-face (A) statistically. Only the means that do not share the same letter are significantly different at a significance level of 0.05.

The *p*-value was used to assess the null hypothesis and determine the statistical significance between the mono-material specimens with and without interface. The null hypothesis states that the means of the population are equal. The criteria to assess the null hypothesis was the significance

level (α) of 0.05 which refers to the 5% risk of false rejection of the hypothesis. The *p*-value which was lower than 0.05 ($p\text{-value} \leq \alpha$) indicates the rejection of the null hypothesis and confirms the significant difference in mechanical properties of a particular design from the monoblock specimen. The results obtained through the *p*-value are in line with the percent variation calculated using the means. The lowest percent variation shown by the overlap (1%) conforms to the highest *p*-value (0.14451) among all designs. The designs with the largest variations from the monoblock specimen have a *p*-value of 0.00001.

A slightly different pattern was identified in the combination of TPU–TPU summarized in Table 5. As shown in Figure 11(a), the maximum ultimate strength was exhibited by the mechanical interlocking (26.5 MPa), followed by the face-to-face interface (24.4 MPa). Also, the strength of the dovetail interface (22.0 MPa) was comparable with the U-shape (21.5 MPa) which can be confirmed by the similar rupture site across the outgoing geometric features. However, a decrease in the strength of the overlap was observed.

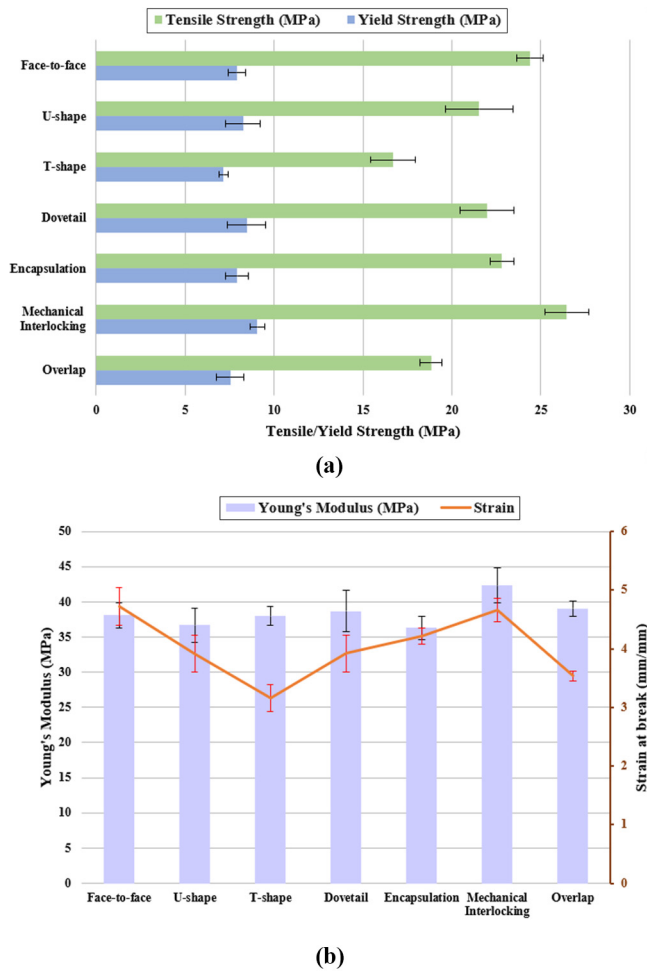
According to Figure 11(a), the yield strength values are significantly lower than the ultimate tensile strength of all interface geometries. The reason is the ductile properties of the TPU material, which is more prone to deformation. The mechanical interlocking tends to have the highest yield strength because of the constriction, which resists deformation and allows the specimens to withstand higher stresses at yield. As for Young's modulus illustrated in Figure 11(b), the values seem to be within the same range. The specimens exhibited ductile behavior because of the mechanical characteristics of TPU. The highest values were shown by mechanical interlocking (42.3 MPa), followed by the T-shape (38.0 MPa)

Table 5 Mechanical properties of the TPU–TPU specimens

Interface geometries	Tensile strength (MPa)			Yield strength (MPa)			Young's modulus (MPa)			Strain at break		
	Mean	SD	Group	Mean	SD	Group	Mean	SD	Group	Mean	SD	Group
Face-to-face	24.4	0.8	A/B	7.9	0.5	A	38.1	1.8	A/B	4.7	0.3	A
U-shape	21.5	1.9	B/C	8.3	1.0	A	36.7	2.5	A/B	3.9	0.3	B
T-shape	16.7	1.2	D	7.1	0.3	A	38.0	1.3	A/B	3.2	0.2	C
Dovetail	22.0	1.5	B/C	8.5	1.1	A	38.7	2.9	A/B	3.9	0.3	B
Encapsulation	22.8	0.7	B	7.9	0.6	A	36.3	1.5	B	4.2	0.1	A/B
Mechanical Interlocking	26.5	1.2	A	9.0	0.4	A	42.3	2.5	A	4.7	0.2	A
Overlap	18.8	0.6	C/D	7.5	0.8	A	39.0	1.0	A/B	3.5	0.08	B/C

Note: Interface geometries that do not share any letter have significantly different means

Figure 11 TPU–TPU specimens



Notes: (a) Tensile and Yield Strength; (b) Young's modulus and Strain

and dovetail (38.7 MPa) interfaces which resulted in a lower elongation at higher stress at break values. This could be attributed to a strong interlocking provided by the abovementioned interfaces, which resist deformation and stretching.

As shown in Table 5, the encapsulation, mechanical interlocking and T-shape do not share the same letter and have statistically significant means for the tensile strength. The yield

strength of all designs shares the letter (A), indicating the insignificant difference between them. Young's moduli of the interfaces also are in the same range with the mechanical interlocking and encapsulation differing substantially. The strains at break of the face-to-face and mechanical interlocking are in the group (A) with a significant difference from the U-shape and dovetail in the group (B) as well as the T-shape (C).

The strain at break of the TPU–TPU specimens [Figure 11(b)] was significantly larger compared to the Tough PLA–Tough PLA because of the flexible nature of the material as expected.

According to Table 6, all TPU geometries also showed a decrease in the values of all mechanical properties compared to mono-material specimens without an interface. In this case, the best geometry is the mechanical interlocking with the lowest variation in terms of the tensile strength (18.6%), yield strength (41.9%) and Young's modulus (5.5%). This design had the second-lowest strain at break variation (13.0%). The lowest variation in the strain at break is shown by the face-to-face interface (12.0%), whereas the highest variation in Young's modulus is seen in the encapsulation interface (18.9%). The least effective interface is T-shape with the highest variation in the tensile strength (48.7%), yield strength (54.1%) and strain at break (41.1%). The *p*-values for Young's modulus of the majority of designs, excluding U-shape and encapsulation, are larger than 0.05, indicating the closeness to the reference monoblock specimen. The results obtained through the *p*-value conform with the percent variation calculated using the means.

3.3 Mechanical properties of multi-material pairs

The values of strain at break for all interface geometries were significantly higher than in the case of Tough PLA–Tough PLA specimens [Figure 12(a)]. Because of the combination of a rigid material with a deformable and flexible one, the specimens demonstrated the elastic behavior of TPU. However, the results presented in Table 7 were substantially lower than the strain of TPU–TPU parts because of the decreased amount of this material. The highest strain values were exhibited by the overlap (1.963). In this particular interface, the connection between materials was maintained by TPU fibers until the fracture occurred. The fibers of the flexible material sustained the link between two parts of the specimen enabling the gradual and considerable elongation of the fibers until reaching the highest strain at break (Fernández et al., 2019). The materials were partially joined at the interface after the rupture. The T-shape geometry also resulted in a high strain at break (0.635) in comparison to the remaining geometries. These results show

Table 6 Effect of the interface geometries on the mechanical properties of mono-material TPU specimens

Interface geometries	Tensile strength		Yield strength		Young's modulus		Strain at break	
	Variation (%)	<i>p</i> -value	Variation (%)	<i>p</i> -value	Variation (%)	<i>p</i> -value	Variation (%)	<i>p</i> -value
Face-to-face	25.0	0.00019	49.3	0.00162	15.0	0.06562	12.0	0.02812
U-shape	33.7	0.00074	46.8	0.00287	18.1	0.04632	27.0	0.00164
T-shape	48.7	0.00005	54.1	0.00101	15.2	0.05765	41.1	0.00011
Dovetail	32.4	0.00041	45.6	0.00355	13.6	0.11045	26.9	0.00153
Encapsulation	29.9	0.00008	49.0	0.00179	18.9	0.03280	21.4	0.00028
Mechanical interlocking	18.6	0.00195	41.9	0.00285	5.5	0.43004	13.0	0.00501
Overlap	42.1	0.00002	51.7	0.00167	12.8	0.08645	34.0	0.00001

Note: The means of interface geometries are compared to the monoblock TPU to obtain the variation percentage and *p*-value

Table 7 Mechanical properties of the multi-material specimens

Interface geometries	Tensile strength (MPa)			Yield strength (MPa)			Young's modulus (MPa)			Strain at break		
	Mean	SD	Group	Mean	SD	Group	Mean	SD	Group	Mean	SD	Group
Face-to-face	3.2	0.4	A	1.13	0.05	A	83.0	5.5	A/B	0.1	0.004	A
U-shape	3.8	0.4	A/B	1.38	0.1	A/B	74.0	3.7	B	0.2	0.05	A
T-shape	5.2	0.3	C	1.42	0.04	B	93.4	5.3	A	0.6	0.05	B
Dovetail	4.2	0.3	B	1.37	0.08	A/B	111.0	4.4	C	0.2	0.02	A
Encapsulation*	19.9	2.1	–	6.99	0.2	–	580.3	58.7	–	0.2	0.02	–
Mechanical interlocking	4.3	0.2	B	1.30	0.03	A/B	124.2	4.3	C	0.1	0.01	A
Overlap	5.6	0.3	C	1.34	0.2	A/B	69.4	6.8	B	2.0	0.2	C

Notes: Interface geometries that do not share any letter have significantly different means

*The encapsulation is separated from the analysis because of its considerably higher mechanical properties

the elastic nature of TPU. The larger deformations were achieved by locking the sections of flexible material with the stiff one. The geometry enabled the elongation and rupture without the TPU section completely slipping away. The T-shape mimics the locking claw system, which allows further deformation of the flexible section (Ribeiro *et al.*, 2018).

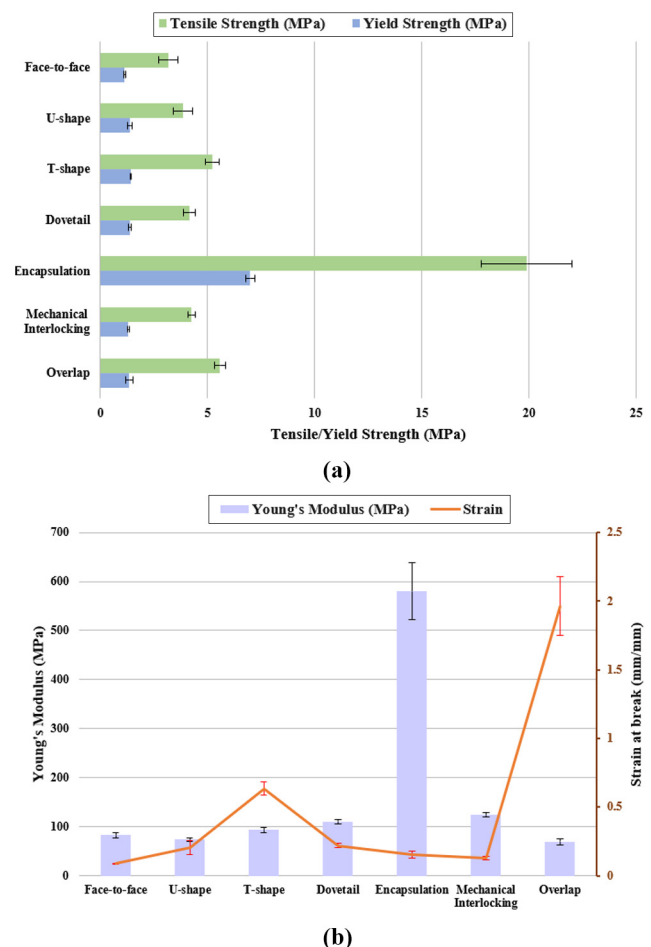
The results of the dovetail specimens (0.220) were close to the U-shape (0.207) while being substantially lower than the T-shape interface (0.635). The dovetail shape relies on both the mechanical and chemical bonding of materials. However, this geometry is not considered a strong locking mechanism to fully restrict the slipping away, while the U-shape interface is a simplified insert that allows failure by detachment (Ribeiro *et al.*, 2018). On the other hand, the mechanical interlocking (0.128) demonstrated a lower strain because of the smaller transition and bonding area. All these three geometries had joint failure caused by the slipping away of the TPU material. The results in the case of the encapsulation indicate that the failure occurred in the vicinity of the jaw where the boundary of materials was located. A negligible amount of TPU traces was found in the dislocated segment of the specimen. The presence of the flexible material was highlighted in the strain (0.153). The elongation of the composite specimen was substantially higher than the corresponding stiff Tough PLA–Tough PLA part. The face-to-face interface had the lowest strain at break (0.089) as expected which agrees with the conclusions of Lopes *et al.* (2018) and Tamburrino *et al.* (2019).

From Figure 12 (b), it can be seen that a significant decrease in the ultimate tensile strength was observed in the multi-material specimens. The drop clearly illustrates the low chemical affinity between Tough PLA and TPU.

All six geometries of multi-material specimens provide a higher tensile strength in comparison to the face-to-face interface specimens (3.19 MPa) which rely only on the chemical affinity of materials for adhesion. This is not the case in the mono-material Tough PLA and TPU specimens with an interface, as the face-to-face geometry demonstrated one of the highest values.

The encapsulation (19.90 MPa) demonstrated the highest ultimate tensile strength. However, the adhesion does not seem as robust as in the case of the overlap and T-shape, as only a small amount of flexible material was still connected to the stiff one. The fracture occurred at the transition region of the Tough PLA and TPU. The next strongest geometries were the overlap (5.59 MPa), followed by the T-shape interface (5.24

Figure 12 Tough PLA–TPU specimens



Notes: (a) Tensile and Yield Strength; (b) Young's modulus and Strain

MPa). The specimens of both geometries had a substantial number of debris of flexible material in the adjacent part after the fracture. It can be observed that the breakage of the specimens occurred at the TPU region because of the higher stiffness and tensile strength of Tough PLA.

The overlap geometry has alternating layers of two materials, which are printed on top of the previous layer. These layers

have higher adhesion and tensile strength because of the interlayer diffusion as observed by Yin *et al.* (2018). Moreover, according to Kim *et al.* (2017), adhesion between the horizontal layers is stronger because of the application of small pressure from the extrusion nozzle to the molten filament during the filament extrusion process. However, the bonding cannot be as robust as in the case of mono-material pairs because of the low compatibility of Tough PLA and TPU.

On the contrary, the U-shape (3.84 MPa), dovetail (4.16 MPa) and mechanical interlocking (4.25 MPa) have slightly lower values of strength. Lower interface strength can be attributed to a smaller cross-sectional area between the two materials, which leads to higher stresses at the joint. Moreover, the small print head movements required to print small design details might result in additional vibrations, which leads to defects at the interface (Hasanov *et al.*, 2020). The sliding out occurred because of the lack of constriction of the geometrical elements of corresponding specimen parts. Therefore, no debris was found at the rupture site with a clean cut between the two materials as depicted in Figure 13. In the case of mono-material Tough PLA and TPU specimens with an interface, these geometries demonstrated more robust bonding. This behavior shows the chemical nature of the bonding in these particular interface designs.

Overall, the interface geometries with the mechanical constriction between materials tend to be more effective choices for higher tensile strength.

Figure 12(b) shows the yield strength of the multi-material specimens. The highest yield strength was exhibited by the encapsulation (6.99 MPa). The reason for this might be the rigid and strong material enveloping the flexible one. The Tough PLA casing undertakes the stress concentrations and enables a higher yield. The other geometries exhibit close values to the face-to-face interface (1.13 MPa) having the lowest yield strength as expected. The yield strength values of the multi-material geometries are substantially lower than the mono-material Tough PLA and TPU with an interface.

As shown in Figure 12(a), a significant drop in Young's modulus is observed for all interfaces compared to both mono-material specimens without and with a boundary interface. This is because of the reduced amount of rigid material. On the contrary, the values of Young's modulus for multi-material parts are higher than the mono-material TPU specimens because of the smaller amount of flexible material leading to a lower strain range. The highest value of Young's modulus was seen in the encapsulation case (580.25 MPa) which was the closest to the mono-material Tough PLA interfaces.

The encapsulation was separated from the analysis, as this design demonstrated considerably higher tensile strength, yield strength and Young's modulus. The T-shape and overlap in the

third group (C) showed significantly higher tensile strength than the dovetail and mechanical interlocking in the second group (B). As for the yield strength, the values were comparatively close resulting in the transitional group (A/B). Regarding Young's modulus, the highest and statistically distinct group (C) included the dovetail and mechanical interlocking. In the case of the strain at break, the T-shape is in the second group (B) with a significant difference from the overlap in the third group (C) as well as all remaining interfaces in the first group (A).

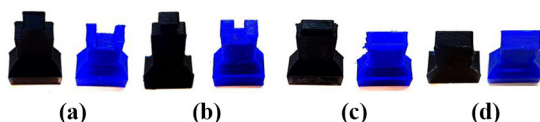
The results seem to be quite reproducible. However, the observed deviations between three specimens of the same design can be attributed to thermal issues as the printer does not have a heated and closed chamber and the internal temperature of the chamber during the printing was not controlled. Therefore, the thermodynamic and diffusion processes for adhesion could be affected (da Silva *et al.*, 2011).

4. Conclusions

In this study, mono-material parts with and without boundary interface, as well as multi-material specimens, were designed and fabricated using FFF (Ultimaker S3). The effect of the existence of the boundary interface and the specific geometries on the structural integrity of the specimens was examined and evaluated. The mechanical properties of the specimens such as tensile strength, yield strength, Young's modulus and strain at break were investigated. Moreover, an analysis of the fracture was performed. The main findings are as follows:

- The failure of the mono-material specimens without a boundary interface of both Tough PLA and TPU occurred at the weakest point which was near the increases of the cross-section.
- As for the mono-material specimens with the interface geometries, the overlap and mechanical interlocking specimens printed using the rigid material failed because of the breakage of geometric elements which indicates the strong adhesion between the parts. The dovetail and U-shape tend to demonstrate the effectiveness of the specimens fabricated using the flexible material. The other geometries fractured near the interface line in both Tough PLA and TPU cases.
- For multi-material interfaces, the overlap and T-shape geometries demonstrated a strong adhesion in comparison to other specimens.
- The analysis of the mechanical properties showed that the presence of the interface line negatively affects the tensile and yield strength of the specimens.
- In the case of the mono-material pairs, the most effective interface designs which showed the lowest variation from the monoblock specimens were the overlap for Tough PLA and the mechanical interlocking for TPU. The encapsulation showed the highest ultimate tensile strength. Nevertheless, the bonding was not as robust as in the case of the overlap and T-shape, as only a small amount of flexible material was still adhered to the stiff one. The interface geometries with the mechanical constriction between materials tend to be more effective choices for better mechanical performance.

Figure 13 Failure by detachment



Notes: (a) U-shape; (b) dovetail; (c) mechanical interlocking; (d) face-to-face interface

Based on this preliminary study, it appears that although these two materials may not be as compatible as other combinations, this composite has a great potential to develop customized shock and vibration absorbers, as the stiffness can be adjusted using Tough PLA and the damping coefficient using TPU.

Multi-material FFF can provide a cost-efficient and competitive way of manufacturing to eliminate the assembly step and reduce the number of components in devices. The applications of the multi-material FFF include components in prosthetics and soft robotics where compliant parts with high strains and the capability of safe interaction with humans are required. Compliant and elastomeric mechanisms can enable rotation, translation and complex motions such as gripping, releasing and jumping (Wallin *et al.*, 2018). Therefore, it is imperative to investigate the mechanical properties. Multi-materials can also decrease the wear of rotating pin and hole parts by fabricating closed structures and can be useful in high-speed devices. Moreover, multi-material combinations, particularly PLA-TPU, can be used in the fabrication of orthoses by providing the trade-off between rigidity and flexibility and improving patient comfort (Venumbaka *et al.*, 2020). Also, multi-material FFF can be useful in printing educational medical models where different materials and color combinations are necessary (Hasanov *et al.*, 2022).

Further investigation into the dynamic response of the composite is needed to confirm these preliminary results.

References

- Amancio-Filho, S. and dos Santos, J. (2009), "Joining of polymers and polymer-metal hybrid structures: recent developments and trends", *Polymer Engineering & Science*, Vol. 49 No. 8, pp. 1461-1476, doi: [10.1002/pen.21424](https://doi.org/10.1002/pen.21424).
- da Silva, L.F., Öchsner, A. and Adams, R.D. (Eds) (2011), *Handbook of Adhesion Technology*, Springer, Heidelberg, doi: [10.1007/978-3-319-55411-2](https://doi.org/10.1007/978-3-319-55411-2).
- Fernández, P., Pelayo, F., Ávila, D., Beltrán, N. and Blanco, D. (2019), "Failure analysis of bi-material FFF parts", *Procedia Manufacturing*, Vol. 41, pp. 571-578, doi: [10.1016/j.promfg.2019.09.044](https://doi.org/10.1016/j.promfg.2019.09.044).
- Hasanov, S., Alkunte, S., Rajeshirke, M., Gupta, A., Huseynov, O., Fidan, I., Alifui-Segbaya, F. and Rennie, A. (2022), "Review on additive manufacturing of Multi-Material parts: progress and challenges", *Journal of Manufacturing and Materials Processing*, Vol. 6, p. 4, doi: [10.3390/jmmp6010004](https://doi.org/10.3390/jmmp6010004).
- Hasanov, S., Gupta, A., Nasirov, A. and Fidan, I. (2020), "Mechanical characterization of functionally graded materials produced by the fused filament fabrication process", *Journal of Manufacturing Processes*, Vol. 58, pp. 923-935, doi: [10.1016/j.jmapro.2020.09.011](https://doi.org/10.1016/j.jmapro.2020.09.011).
- Jasveer, S. and Jianbin, X. (2018), "Comparison of different types of 3D printing technologies", *International Journal of Scientific and Research Publications*, Vol. 8 No. 4, pp. 1-9, doi: [10.29322/IJSRP.8.4.2018.p7602](https://doi.org/10.29322/IJSRP.8.4.2018.p7602).
- Kim, H., Park, E., Kim, S., Park, B., Kim, N. and Lee, S. (2017), "Experimental study on mechanical properties of single- and dual-material 3D printed products", *Procedia Manufacturing*, Vol. 10, pp. 887-897, doi: [10.1016/j.promfg.2017.07.076](https://doi.org/10.1016/j.promfg.2017.07.076).
- Kuipers, T., Su, R., Wu, J. and Wang, C.C.L. (2022), "ITIL: interlaced topologically interlocking lattice for continuous dual-material extrusion", *Additive Manufacturing*, Vol. 50, p. 102495, doi: [10.1016/j.addma.2021.102495](https://doi.org/10.1016/j.addma.2021.102495).
- Lin, W., Shen, H., Xu, G., Zhang, L., Fu, J. and Deng, X. (2018), "Single-layer temperature-adjusting transition method to improve the bond strength of 3D-printed PCL/PLA parts", *Composites Part A: Applied Science and Manufacturing*, Vol. 115, pp. 22-30, doi: [10.1016/j.compositesa.2018.09.008](https://doi.org/10.1016/j.compositesa.2018.09.008).
- Lopes, L.R., Silva, A.F. and Carneiro, O.S. (2018), "Multi-material 3D printing: the relevance of materials affinity on the boundary interface performance", *Additive Manufacturing*, Vol. 23, pp. 45-52, doi: [10.1016/j.addma.2018.06.027](https://doi.org/10.1016/j.addma.2018.06.027).
- Minitab (2021), "Interpret the key results for One-Way ANOVA", available at: <https://support.minitab.com/en-us/minitab/21/help-and-how-to/statistical-modeling/anova/how-to/one-way-anova/interpret-the-results/key-results/> (accessed 21 November 2022).
- Minitab (2022), "What is Tukey's method for multiple comparisons?", available at: <https://support.minitab.com/en-us/minitab/21/help-and-how-to/statistical-modeling/anova/supporting-topics/multiple-comparisons/what-is-tukey-s-method/> (accessed 21 November 2022).
- Nace, S.E., Tiernan, J., Holland, D. and Annaidh, A.N. (2021), "A comparative analysis of the compression characteristics of a thermoplastic polyurethane 3D printed in four infill patterns for comfort applications", *Rapid Prototyping Journal*, Vol. 27 No. 11, pp. 24-36, doi: [10.1108/RPJ-07-2020-0155](https://doi.org/10.1108/RPJ-07-2020-0155).
- Ribeiro, M., Sousa Carneiro, O. and Ferreira da Silva, A. (2018), "Interface geometries in 3D multi-material prints by fused filament fabrication", *Rapid Prototyping Journal*, Vol. 25 No. 1, pp. 38-46, doi: [10.1108/RPJ-05-2017-0107](https://doi.org/10.1108/RPJ-05-2017-0107).
- Stoner, B., Bartolai, J., Kaweesa, D.V., Meisel, N.A. and Simpson, T.W. (2018), "Achieving functionally graded material composition through bicontinuous mesostructural geometry in material extrusion additive manufacturing", *Journal of the Minerals, Metals & Materials Society*, Vol. 70, pp. 413-418, doi: [10.1007/s11837-017-2669-z](https://doi.org/10.1007/s11837-017-2669-z).
- Tamburrino, F., Graziosi, S. and Bordegoni, M. (2019), "The influence of slicing parameters on the multi-material adhesion mechanisms of FDM printed parts: an exploratory study", *Virtual and Physical Prototyping*, Vol. 14 No. 4, pp. 316-332, doi: [10.1080/17452759.2019.1607758](https://doi.org/10.1080/17452759.2019.1607758).
- Ultimaker (2023a), "Ultimaker Tough PLA material: create durable prototypes and tooling", available at: <https://ultimaker.com/materials/tough-pla> (accessed 20 April 2022).
- Ultimaker (2023b), "Ultimaker TPU 95A material: 3D print durable and flexible parts", available at: <https://ultimaker.com/materials/tpu-95a> (accessed 20 April 2022).
- Venumbaka, S.A., Covarubias, M., Cesaro, G., Ronca, A., De Capitani, C., Ambrosio, L. and Sorrentino, A. (2020), "Application of multi materials additive manufacturing technique in the design and manufacturing of hand orthoses", *Proceedings of the International Conference on Computers Helping People with Special Needs LNCS, Lecco*,

- Italy*, Vol. 12377, pp. 461-468, doi: [10.1007/978-3-030-58805-2_55](https://doi.org/10.1007/978-3-030-58805-2_55).
- Vu, I.Q., Bass, L.B., Williams, C.B. and Dillard, D.A. (2018), "Characterizing the effect of print orientation on interface integrity of multi-material jetting additive manufacturing", *Additive Manufacturing*, Vol. 22, pp. 447-461, doi: [10.1016/j.addma.2018.05.036](https://doi.org/10.1016/j.addma.2018.05.036).
- Wallin, T.J., Pikul, J. and Shepherd, R.F. (2018), "3D printing of soft robotic systems", *Nature Reviews Materials*, Vol. 3, pp. 84-100, doi: [10.1038/s41578-018-0002-2](https://doi.org/10.1038/s41578-018-0002-2).
- Yin, J., Lu, C., Fu, J., Huang, Y. and Zheng, Y. (2018), "Interfacial bonding during multi-material fused deposition

- modeling (FDM) process due to inter-molecular diffusion", *Materials & Design*, Vol. 150, pp. 104-112, doi: [10.1016/j.matdes.2018.04.029](https://doi.org/10.1016/j.matdes.2018.04.029).
- Zheng, Y., Zhang, W., Baca Lopez, D.M. and Ahmad, R. (2021), "Scientometric analysis and systematic review of multi-material additive manufacturing of polymers", *Polymers*, Vol. 13 No. 12, pp. 1-33, doi: [10.3390/polym13121957](https://doi.org/10.3390/polym13121957).

Corresponding author

Didier Talamona can be contacted at: didier.talamona@nu.edu.kz